TripleA: Accelerated Accuracy-preserving Alignment for Iris-Codes

Christian Rathgeb[1] • Heinz Hofbauer[2] • Christoph Busch[2] • Andreas Uhl[1]

[1]da/sec – Biometrics and Internet Security Research Group, Hochschule Darmstadt, Germany,
{christian.rathgeb,christoph.busch}@h-da.de
[2]Multimedia Signal Processing and Security Lab, University of Salzburg, Austria, {hhofbaue,uhl}@cosy.sbg.ac.at

Abstract

The discriminative power of the iris enables reliable biometric recognition on large-scale databases where a rapid comparison of biometric reference data is essential to limit response times. In case of national-sized databases a one-to-many comparison might still represent a bottleneck of a biometric identification system, in particular if numerous relative tilt angles have to be considered in the comparisons stage. While a compensation of head tilts improves the robustness of an iris recognition system, extensive feature alignment increases the probability of a false match as well as comparison time.

In this paper we present a novel method to accelerate iris biometric comparators in an accuracy-preserving way. Emphasis is put on the alignment of iris biometric reference data, i.e. iris-codes. Based on an analysis of the nature of iris-codes and comparison scores between them we propose an efficient two-step alignment process referred to as TripleA. This scheme, which can be operated in various modes, significantly reduces the amount of relative tilt angles to be considered during iris-code comparisons. Hence, comparison time as well as the probability of a false match are reduced at the same time. In an experimental evaluation on the Casia v4-Interval iris database we achieve a more than fourfold speed-up in the comparison stage maintaining biometric performance using different feature extraction techniques.

Contents

1 Introduction

Due to its rich random structure, and hence its resistance to false matches, the iris represents one of the most powerful biometric characteristics [1–3]. Deployments of iris recognition technologies in numerous large-scale nation-wide projects mark its tremendous inroads [4]. Following Daugman's approach [1], which is the core of most public operational deployments, four major modules constitute an iris recognition system: (1) image acquisition, where most current deployments require subjects to fully cooperate with the system in order to capture images of sufficient quality; (2) pre-processing, which includes the detection of the pupil and the outer iris boundary. Subsequently, the iris (approximated in the form of a ring) is normalized to a rectangular texture on which image enhancement methods, e.g. histogram stretching, are applied. To complete the preprocessing, parts of the iris texture which are occluded by eye-lids, eye-lashes or reflections are detected and stored in an according noise-mask; (3) feature extraction, in which a binary feature vector, i.e. iris-code, is generated by applying adequate filters to the pre-processed iris texture. This binary data representation enables compact storage and rapid (4) comparison, which is based on the estimation of Hamming distance (*HD*) scores between pairs of iris-codes and corresponding masks, achieving millions of comparisons per second per CPU core [1].

In the comparison stage circular bit shifts are applied to iris-codes and *HD* scores are estimated at K different shifting positions, i.e. relative tilt angles. The minimal obtained *HD*, which corresponds to an optimal alignment, represents the final score. Hence, score distributions are skewed towards lower *HD* scores, which (for a given threshold) increases the probability of a false match by the factor K [5]. It is important to note, that the number of shifting positions employed to determine an appropriate alignment between pair of iris-codes may vary depending on the application scenario. Some public deployments of iris recognition go as far as $K = 21$ shifting positions when handheld cameras are used for which it is obviously more difficult to ensure an upright capture orientation [5], increasing the computational effort of a single pair-wise comparison of iris-codes by the factor K. In biometric identification systems exhaustive $1 : N$ comparisons are required in order to identify a biometric probe, where N represent the number of subjects registered with the system. In case large values of K are unavoidable, the time required for a single identification will significantly increase, since comparison time dominates the overall computational workload in any large-scale biometric identification system [6].

In past years, different concepts have been proposed in order to accelerate iris biometric (identification) systems (see Sect. 2). However, apart from hardware-based parallelization [7, 8], presented schemes either fail to provide a significant acceleration or they suffer from a significant decrease in recognition accuracy. Hence, existing approaches often obtain a trade-off between biometric performance (recognition accuracy) and speed-up compared to a traditional iris recognition system. Furthermore, in practise most concepts do not allow for a seamless integration into a conventional identification system.

In this work, we propose a novel technique for comparing pairs of iris-codes, which we refer to as Accelerated Accuracy-preserving Alignment – *TripleA*. In contrast to related works which also aim at a software-based acceleration of iris recognition systems, e.g. [6, 9], focus is put on the alignment process. Based on an analysis of *HD* scores obtained at different shifting positions during genuine iris-code comparisons we introduce an adjustable two-step search-procedure in order to efficiently determine alignments between iris-codes. Within the proposed procedure only a fraction of K shifting positions has to be considered during a single pair-wise comparison, while covering the same range of possible tilt angles. Experiments confirm that the proposed scheme is capable of obtaining a more than four-fold speed-up for different feature extraction algorithms. At the same time biometric performance is maintained even though in a few cases the obtained alignments might only turn out near-optimal, since the probability of a false match (just by chance) is significantly lowered by the number of considered shifting positions.

This paper is organized as follows: Sect. 2 briefly summarizes key concepts for acceleration of iris biometric (identification) systems. In Sect. 3 the proposed system is described in detail. Experimental evaluations are presented in Sect. 4. Finally, conclusions are drawn in Sect. 5.

2 Related Work

With respect to workload reduction in biometric (identification) systems, we might differentiate between four key concepts: (1) hardware-based acceleration, (2) indexing, (3) coarse classification or "binning", and (4) a serial combination of a computationally efficient and an accurate (but more complex) algorithm. Let ω be the workload for a single iris-code comparison and $\mathcal{W} = \omega N$ that of a $1 : N$ comparison, which frequently dominates the overall computational workload of an iris biometric identification system.

Adapting comparison procedures to adequate hardware, e.g. multiple cores within a CPU or a GPU, allows for parallelization [7]. By simultaneously executing a number of t threads $\mathcal{W}$ can be reduced to $\omega N/t$ since a $1 : N$ comparison can be performed in parallel on t subsets of equal size N/t. As pointed out by Vandal and Savvides [8], the number of considered shifting positions K represents a crucial factor which might significantly decrease the throughput of the system. However, the estimation of *HD* scores at various shifting positions during alignment can be parallelized as well.

Biometric indexing aims at reducing the overall workload of a biometric identification attempt in terms of $\mathcal{O}$-notation, where existing approaches focus on reducing the workload to at least $\mathcal{O}(\log N)$, yielding $\mathcal{W} = \omega \log N$. In the majority of cases this is achieved by introducing hierarchical search structures which tolerate a distinct amount of biometric variance. Most notably, Hao *at al.* [6] proposed a search algorithm for iris-codes based on Beacon Guided Search combining a multiple colliding segments principle and early termination

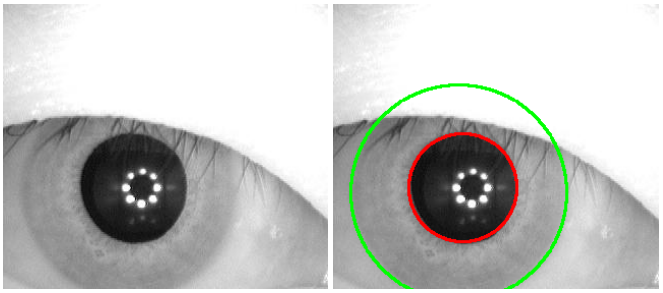

(a) Iris image (b) Iris segmentation

(c) Pre-processed iris texture

(d) LG iris-code - real and imaginary filter response

(e) QSW iris-code - split by wavelet subband response

Figure 1: Iris biometric processing chain for image S1234R01 of the Casia v4–Interval database.

strategy. The technique is evaluated using 632,500 iris-codes enrolled in the United Arab Emirates (UAE) border control system, showing a substantial improvement in search speed with a negligible loss of accuracy. More recently, Proença [10] presented an iris indexing scheme designed for unconstrained scenarios. In a comparative evaluation the scheme is shown to outperform existing schemes, e.g. [6], on degraded iris images of the UBIRISv2 database. Rathgeb *at al.* [11] proposed an indexing scheme based on a hierarchical Bloom filter structure into which iris-codes are mapped. On the IITDv1 iris database identification rates of a conventional identification scheme were maintained providing a retrieval in $\mathcal{O}(\log N)$ steps. Further, approaches to iris indexing in the image domain have been proposed [12, 13]. While most works report hit/penetration rates on distinct datasets, required computational efforts are frequently omitted. The application of complex search structures on rather small datasets may cloud the picture about actual gains in terms of speed and leaves scalability of some approaches doubtful.

By binning an iris biometric database into c classes, $\mathcal{W}$ can be reduced to $\omega N/c$, given that irises of registered subjects are equally distributed among these classes. While other biometric characteristics suggest a natural pre-classification, e.g. standard types of fingerprints, for iris only eye color has been considered for visible wavelength iris images [14, 15]. However, recent advances in the field of soft biometrics might enable a binning of iris images with respect to age or ethnicity classes (for further details on soft biometrics the reader is referred to [16]).

Within serial combinations computationally efficient algorithms are used to extract a short-list of $\mathcal{L}N$ most likely candidates, with $\mathcal{L} \ll 1$. Therefore, $\mathcal{W}$ is reduced to $\hat{\omega}N + \omega\mathcal{L}N$, where $\hat{\omega}$ is the workload of a pair-wise comparison of the computationally efficient algorithm, with $\hat{\omega} \ll \omega$. In other words, identification is accelerated if $\omega(1-\mathcal{L}) > \hat{\omega}$ holds. For instance, Gentile *at al.* [9] reduced $\mathcal{L}$ to ∼10% employing compressed versions of original iris-codes during pre-screening. Thereby, the overall number of required bit-comparisons was significantly reduced.

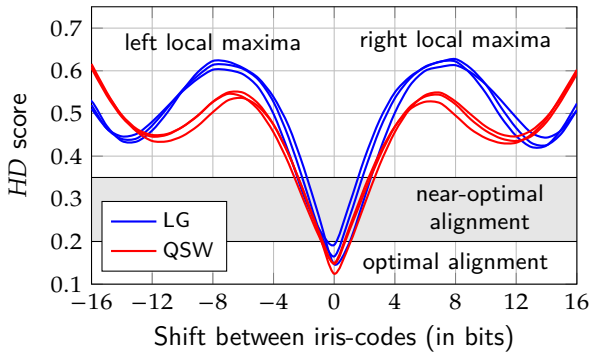

Figure 2: Sample HD-scores obtained from three genuine pairs of iris-codes at various shifting positions.

3 Proposed System

In the following subsections we summarize the baseline iris recognition system and present some analysis of *HD* scores estimated from genuine iris-code comparisons across various shifting positions. Based on this analysis we propose the adjustable two-step search-procedure, *TripleA*, in order to align pairs of iris-codes in an efficient and accuracy-preserving manner.

3.1 Setup and Analysis

In the employed iris recognition system the iris of a given sample image is detected and transformed to a rectangular texture of 512 × 64 pixel applying a contrast-adjusted Hough transform. In the feature extraction stage two conventional algorithms are employed where normalized enhanced iris textures are divided into stripes to obtain 10 one-dimensional signals, each one averaged from the pixels of 5 adjacent rows (the upper 512×50 rows are analysed). The first feature extraction method follows the Daugman-like 1D-LogGabor feature extraction algorithm of Masek [17] (LG) and the second follows the algorithm proposed by Ma *et al.* [18] (QSW) based on a quadratic spline wavelet transform. Both feature extraction techniques generate iris-codes of B= 512×20 = 10,240 bit. Fig.1 illustrates the described processing chain for a sample iris image resulting in different types of iris-codes. Custom implementations of employed segmentation and feature extractors are freely available in the University of Salzburg Iris Toolkit (USIT) [19]. For further details on the employed feature extraction algorithms the reader is referred to [2].

For both feature extraction algorithms Fig. 2 depicts the *HD* scores across various shifting positions for three genuine comparisons of iris-codes. For the described system a 1-bit shift equals 0.7° of rotation. It can be observed that for each feature extractor the *HD* scores of the three genuine comparisons

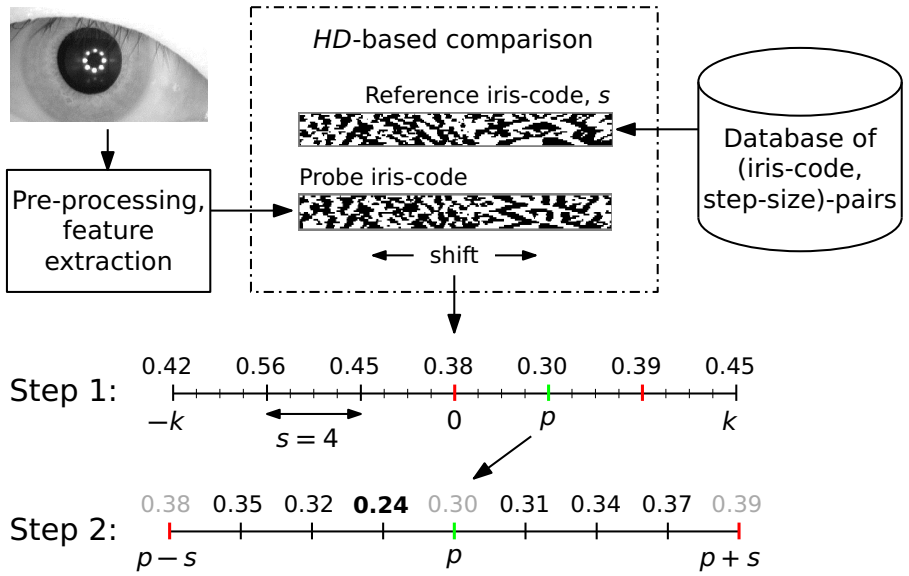

Figure 3: Example of the *TripleA* procedure in *dynamic* mode: In the first step comparisons between a probe and reference iris-code are performed at $2k/s + 1 = 7$ positions according to the reference's step size $s = 4$. After detecting the near-optimal shifting position $p = 4$, the final score (marked bold) is detected in the interval $[p - s + 1 = 1; p + s - 1 = 7]$ at a shifting position of 3. *HD* scores are estimated at a total number of 13 shifting positions compared to $K = 25$ in a linear search.

seem almost identical. Within a certain range *HD* scores constantly decrease towards the minimum (best) score. This range is enclosed by local maxima yielding *HD* scores significantly beyond 0.5. For the sample *HD* scores in Fig. 2 these local maxima can be found at shifting positions of ± 8 bits for LG and ± 6 bits for QSW. This phenomenon can be explained by taking account of two key observations:

1. Daugman has shown that bits in iris-code are not mutually independent [1], also see Fig. 1 (d)-(e). In order to measure 'iris-code entropy' it is suggested to estimate the degrees of freedom (*DoF*) provided by iris-codes. Using a Bernoulli model the number of mutual independent bits is obtained from imposter score distribution as $DoF = (\mu(1-\mu))/\sigma^2$, where μ and σ^2 denote the mean and variance. In other words, iris-codes can be modelled as sticky oscillators [5].
2. Hollingsworth *at al.* [20] have shown, that for ideal imaging (no eyelash/eyelid occlusions, corneal reflections, etc. on iris textures) so-called "fragile" bits, i.e. bits which exhibit a higher probability than others to flip their value during a genuine comparison, most likely occur between consecutive 1-bit and 0-bit sequences. Since filters employed in the feature extraction stage set iris-code bits by their sign, fragile bits correspond to coefficients close to zero.

Given the first observation, rows of iris-codes can be expected to consist of consecutive 1-bit and 0-bit sequences rather than of random sequential bits. Based on the second observation we conclude that the number of bit-sequence flanks, i.e. changes from 1-bit to 0-bit sequences and vice versa, remains rather constant for genuine iris-codes since bit-flips are expected to occur between sequences. Hence, the average length of 1-bit and 0-bit sequences μ_s can be expected to remain stable as well. Intuitively, the distance between the shifting position resulting in a minimum *HD* score and those of surrounding local *HD* score maxima might be approximated by μ_s, as $\pm\mu_s$ bit shifts are expected to cause the most drastic misalignment. The sequence of *HD* scores between genuine iris-codes across different shifting positions might be interpreted as an oscillation which decreases its amplitude with the distance to the minimum score. For such a signal it can be empirically verified that distances between consecutive vertices are virtually the same for a constant value of μ_s even in case of large standard deviations.

3.2 Accelerated Accuracy-preserving Alignment

The proposed *TripleA* approach comprises the following two key steps: (1) estimation of near-optimal alignment and (2) estimation of subset-minimum. An example of the approach is illustrated in Fig. 3.

In the first step the range of $K = 2k + 1$ shifting positions $[-k; k]$ is divided into $2k/s$ intervals, where s denotes the employed *step-size*. Then *HD* scores are estimated at interval boundaries, i.e. for a subset of $2k/s + 1$ shifting positions. In other words, the sequence of scores, interpreted as signal, is sampled every s bits. Based on the above observations for a genuine comparison a sampling with at most the average length of 1-bit and 0-bit sequences, $s < \mu_s$, is expected to detect a minimum score which represents a near-optimal alignment. We consider an alignment as near-optimal if the corresponding shifting position is close enough to the optimal alignment revealing a *HD* score which is significantly smaller compared to remaining sampling positions. For the sample comparisons of Fig. 2 near-optimal alignments would be found in the range of approximately ± 2 bit shifts.

After detecting a near-optimal alignment at shifting position p the interval $[p - s + 1; p + s - 1]$ is considered for the second step. Note that the scores for positions $p \pm s$ have al-

ready been estimated in the first step. Based on a linear search the second step detects a minimum *HD* score for a subset of $2(s-1)$ shifting positions.

The proposed *TripleA* scheme can be operated in two modes, defined by the estimation of the step-size:

1. *Static Mode*: A static value of s is used for each comparison performed by the system. In this case μ_s can be averaged from a training set of extracted iris-codes. Another way to estimate an upper bound for s would be to analyse the provided *DoF*. Therefore, *DoF* has to be averaged from a line-wise analysis of R iris code rows resulting in $DoF_R = 1/R \sum_{i=1}^{R} DoF_i$, where DoF_i denotes the *DoF* provided by line i. Thereby, correlation between different rows of iris-codes is suppressed so that B/DoF_R serves as an adequate upper bound for s, where B is the number of bits in the iris-code.
2. *Dynamic Mode*: The step-size s is estimated dynamically for a single reference iris-code during enrolment. Hence, μ_s is estimated from a single iris-code and the step size is defined as $c\mu_s$ with $0 < c \leq 1$. At the time of authentication a probe iris-code is compared against a reference iris-code applying the corresponding step size stored with the latter. Even though, μ_s is expected to exhibit a larger standard deviation when estimated from a single iris-code, different values of μ_s might serve as further feature of iris-codes.

In the general *TripleA* approach the number of shifting positions to be considered is reduced to $C = \lceil K/s \rceil + 1 + 2(s-1) \approx K/s + 2s$. To obtain a maximum speed-up C has to be minimized. By setting the derivative $\frac{d}{ds}C = 2 - K/s^2 = 0$ we get $s = \sqrt{K}/\sqrt{2}$ as optimal step-size in terms of speed-up. To further accelerate the proposed alignment we suggest two derivations of *TripleA*:

- *TripleA - Limited*: In this setting the first step is only applied on a defined upper parts of two iris-codes. Thereby, only a fraction of bit comparisons is required in the first step while in the second step the minimum *HD* score is estimated from all $2s+1$ shifting positions of the subset.
- *TripleA - Single-sided*: Building upon *TripleA - Limited* only half of the subset detected in the first step is considered during the second step. This bisected interval is defined by p and minimum of surrounding *HD* scores at $p \pm s$. In the example of Fig. 3 the interval $[p-s+1, p-1]$ would be chosen for the linear search of the second step, since the *HD* score at shifting position $p-s$ is smaller than that at $p+s$.

It is important to note, that the proposed derivations build upon observations made for genuine iris-code comparisons. Obviously, *HD* scores across different shifting positions do not show the same behaviour for impostor comparisons. This means that the TripleA derivations are likely to reduce the probability of false matches for impostor comparisons due to finding suboptimal alignments for impostors.

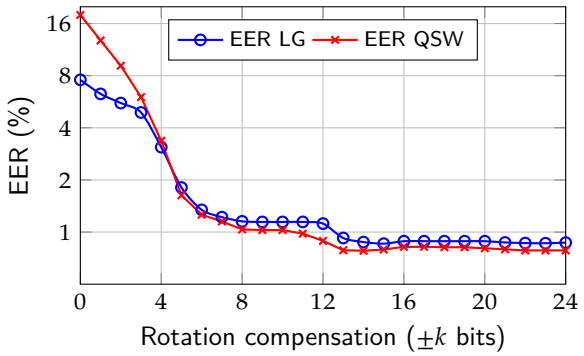

Figure 4: Progression of EERs in relation to rotation compensation: in a linear search *HD* scores are estimated for $\pm k$ shifting positions.

Rot. comp.	LG		QSW	
$\pm k$ bits	EER	$FNMR_{0.01}$	EER	$FNMR_{0.01}$
0	7.57	14.62	17.94	24.52
1	6.28	13.09	12.78	18.22
2	5.56	12.41	9.13	13.65
4	3.09	12.07	3.37	7.52
8	1.15	2.76	1.04	1.76
12	1.12	2.72	0.88	1.55
16	**0.89**	**2.14**	**0.82**	**1.27**
20	0.89	2.14	0.81	1.26
24	0.87	2.08	0.78	1.22

Table 1: Progression of EERs and $FNMR_{0.01}$s in relation to rotation compensation (results of baseline settings are marked bold).

4 Experiments

Experimental evaluations are carried out on the Casia v4-Interval iris database [21]. The database consists of 2,639 good-quality 320×280 pixel NIR iris images of 249 subjects. In accordance with IS ISO/IEC 19795-1:2006 [22] biometric performance is estimated in terms of false non-match rate (FNMR) at a target false match rate (FMR) and equal error rate (EER) obtained from performing all 3,480,841 iris-code cross-comparisons. When averaging row-wise estimations of *DoF*, DoF_R values of 1,587.80 (LG) and 2,458.97 (QSW) are obtained, neglecting correlation between iris-code rows. Hence, for the LG and QSW algorithm B/DoF_R would yield upper bounds of approximately 6 and 4 for step-sizes, respectively.

The difference in step-size highlights the use of redundancies within iris-codes. There is a substantial likelihood of neighbouring iris-code bits being equal as these originated from overlapping filter responses obtained from neighbouring texture parts of an iris texture [5]. For LG these bits correspond to the signs of a 1D-LogGabor wavelet response. QSW on the other hand encodes extrema in the filter responses of a quadratic spline wavelet, leading to a varying degree of overlap which requires smaller step-sizes in the proposed approach.

In a first experiment we calculate EERs and FNMRs at a FMR of 0.01%, $FNMR_{0.01}$, considering $\pm k$ shifting positions during alignment performing a linear search for the minimum *HD* score. The progress in terms of EER with respect to rotation compensation is plotted in Fig. 4. Table 1 summarizes

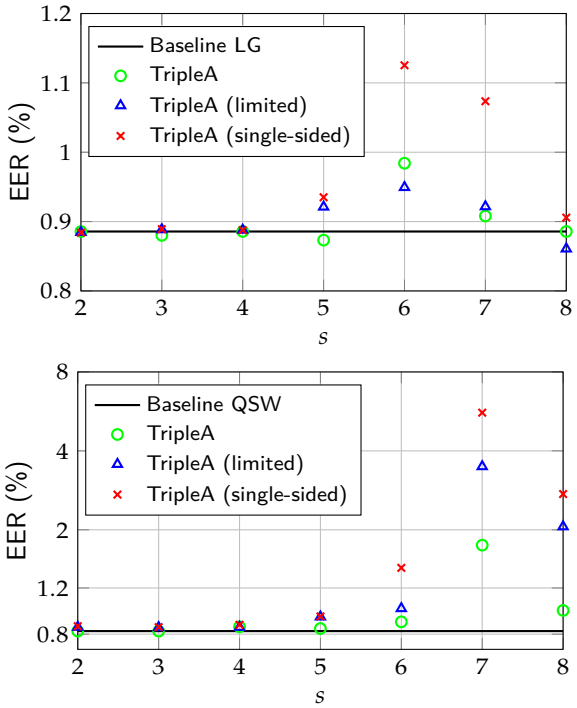

Figure 5: EERs of the proposed approaches for different static step-sizes for the LG (top) and QSW (bottom) feature extraction (note different scales on y-axes).

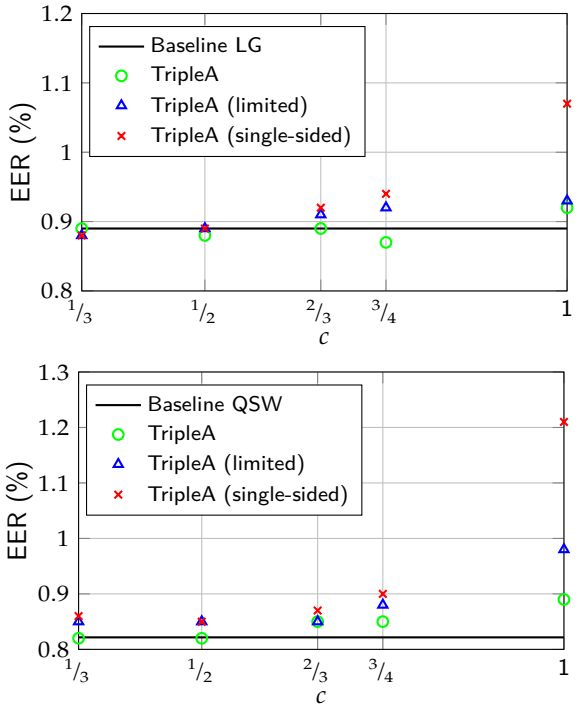

Figure 6: EERs of the proposed approaches for different dynamic step-sizes of $s = c\mu_s$ for the LG (top) and QSW (bottom) feature extraction.

obtained EERs and $\text{FNMR}_{0.01}$s. As can be seen the majority of misalignments is compensated by ± 8 bit shifts ($\sim 6°$) while biometric performance converges at approximately ± 16 bit shifts ($\sim 11°$). Focusing on recognition accuracy versus required bit-shifting we choose $k = 16$, i.e. $K = 33$, as reasonable trade-off for our baseline systems resulting in practical an EER of 0.89% and a $\text{FNMR}_{0.01}$ of 2.14% for LG and an EER of 0.82% and a $\text{FNMR}_{0.01}$ of 1.27% for QSW.

Iris-codes are internally represented as two-dimensional arrays consisting of $B/8$ bytes (chars). *HD* scores are estimated by successively XORing bytes and counting the bits set within resulting bytes via a 8-bit look-up table. The implementation can be considered lightweight and fully portable as it does not make use of larger look-up tables which require a significant amount of RAM nor of CPU-specific PopCnt (population count) functions. Nevertheless, it is important to note that achieved relative speed-ups directly apply to any more sophisticated comparison engine which might make large use of intrinsic functions, parallelization, etc.

In the following subsection we evaluate the biometric performance and provided speed-up of the proposed *TripleA* approaches.

4.1 Performance Evaluation

For different configurations of *TripleA* and step-sizes in static and dynamic mode, comparisons of obtained EERs to the according baseline systems are plotted in Fig. 5 and Fig. 6, respectively. We observe that for the static mode the pre-estimated assumption $s < B/DoF_R$ is reasonable since EERs turn out to significantly increase for static step-sizes of approximately 6 for LG and 4 for QSW (note the log-scale for the bottom plot of Fig. 5). Moreover, it can be seen that for some configurations, in particular for the LG feature extraction, biometric performance is slightly improved in both modes. These improvements occur due to the previously mentioned fact that impostor distributions are skewed towards larger *HD* scores. For a sample configuration this effect is illustrated in Fig. 7. It can be observed, that the vast majority of genuine scores remains equal compared to the baseline system while imposter distributions shifted towards larger *HD* scores. Focusing on biometric performance this effect compensates potential alignment errors.

With respect to the dynamic mode the according relative frequencies of average sequence lengths, μ_ss, are plotted in Fig. 8. For the LG feature extraction average sequence lengths are longer than those obtained for the QSW feature extraction which coincides with previous *DoF* estimations for both algorithms. Table 2 summarizes obtained EERs and $\text{FNMR}_{0.01}$s for all configurations of the proposed TripleA approach. For the general approach it can be observed that in both modes, using static and dynamic step sizes, biometric performance is maintained across most step-size settings.

For the LG feature extraction neither the *limited* nor the *single-sided* setting causes a drastic decrease in accuracy while these approaches provide substantial further speed-ups as will be shown in the following subsection. In contrast, for the QSW feature extraction biometric performance significantly decreases for the *limited* and *single-sided* setting in the static mode using step-sizes of $s \geq 6$. That is, for QSW the search for a near-optimal alignment on the upper 512×8 bits of iris-codes as well as a single-sided interval choice turn out to be more error-prone compared to LG. For the dynamic mode step-size

Mode	Step size	TripleA				TripleA - limited				TripleA - one-sided			
		LG		QSW		LG		QSW		LG		QSW	
		EER	$FNMR_{0.01}$	EER	$FNMR_{0.01}$	EER	$FNMR_{0.01}$	EER	$FNMR_{0.01}$	EER	$FNMR_{0.01}$	EER	$FNMR_{0.01}$
Static	2	0.89	2.14	0.82	1.27	0.88	2.18	0.85	1.40	0.88	2.18	0.86	1.40
	3	0.88	2.13	0.82	1.28	0.89	2.22	0.85	1.41	0.89	2.20	0.85	1.41
	4	0.89	2.17	0.85	1.37	0.89	2.19	0.85	1.56	0.89	2.19	0.87	1.57
	5	0.87	2.17	0.84	1.33	0.92	2.24	0.93	1.49	0.94	2.24	0.93	1.55
	6	0.98	3.30	0.89	1.58	0.95	2.70	1.00	2.10	1.13	3.57	1.43	2.46
	7	0.91	2.42	1.75	2.49	0.92	2.46	3.48	4.56	1.07	3.63	5.59	8.70
	8	0.89	2.17	0.99	1.54	0.86	2.17	2.74	2.78	0.91	2.32	2.05	6.58
Dyn.	$^1/_3\,\mu_s$	0.89	2.14	0.82	1.27	0.88	2.18	0.85	1.38	0.88	2.18	0.86	1.39
	$^1/_2\,\mu_s$	0.88	2.14	0.82	1.28	0.89	2.22	0.85	1.41	0.89	2.20	0.85	1.41
	$^2/_3\,\mu_s$	0.89	2.17	0.85	1.36	0.91	2.20	0.85	1.53	0.92	2.19	0.87	1.53
	$^3/_4\,\mu_s$	0.87	2.17	0.85	1.37	0.92	2.24	0.88	1.56	0.94	2.25	0.90	1.57
	μ_s	0.92	2.57	0.89	1.53	0.93	2.45	0.98	1.89	1.07	3.60	1.21	2.75

Table 2: EERs and $FNMR_{0.01}$ for different settings of *TripleA* for the static and dynamic modes for the LG and QSW feature extraction (LG baseline: EER=0.89%, $FNMR_{0.01}$=2.14%; QSW baseline: EER=0.82%, $FNMR_{0.01}$=1.27%).

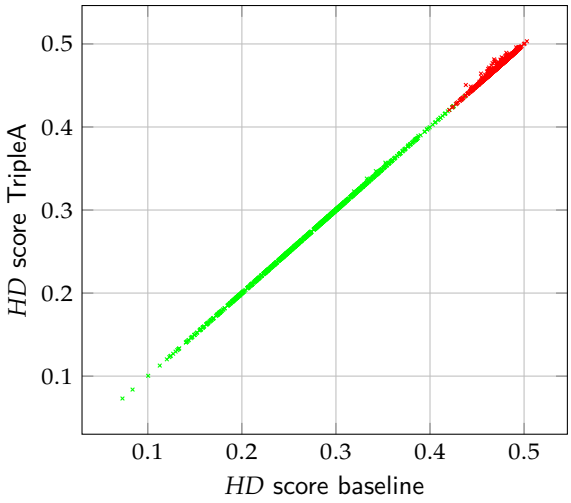

Figure 7: Scatter plot for 1000 genuine (in green) and impostor (in red) comparisons performed by the baseline comparator and TripleA in dynamic mode with a step-size $s = 0.5\mu_s$ for LG feature extraction.

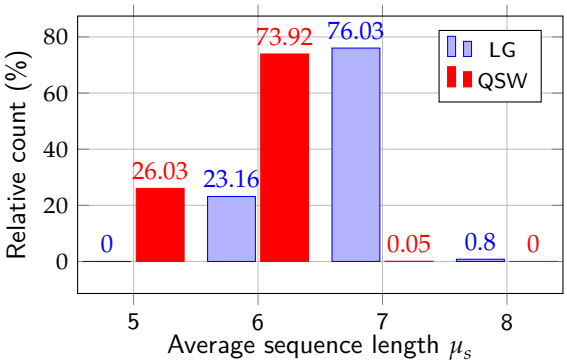

Figure 8: Relative frequencies of average sequence lengths used in dynamic mode for LG and QSW feature extraction.

of $s \leq 2/3\mu_s$ appear most suitable for both feature extraction methods.

4.2 Timing Tests

All experiments were performed on a single core of an Intel Core i7-3610QM CPU with 3.2GHz on a standard work station with sufficient RAM. A single comparison of iris-codes takes ~100 micro seconds for the above described (non-optimized) baseline comparator. Relative speed-ups provided by proposed *TripleA* approaches are summarized in Table 3 (note that speed-ups are equal for both feature extractors since iris-codes are of same size and dimension). As previously mentioned, a higher step-size is not necessarily optimal. For the search space of $K = 2 \cdot 16 + 1 = 33$ an optimal speed-up is achieved for $s = \sqrt{33}/\sqrt{2} = 4$. For the general *TripleA* approach this results in an almost two-fold speed-up compared to the baseline system while larger step-sizes reveal lower speed-ups.

Mode	Step-size	TripleA	TripleA limited	TripleA one-sided
Static	2	1.6	3.8	4.4
	3	1.7	3.4	4.6
	4	1.9	3.0	4.6
	5	1.7	2.6	4.1
	6	1.7	2.3	3.9
	7	1.5	2.0	3.5
	8	1.5	1.8	3.3
Dyn.	$^1/_3\,\mu_s$	1.6	3.8	4.4
	$^1/_2\,\mu_s$	1.7	3.4	4.6
	$^2/_3\,\mu_s$	1.9	3.0	4.6
	$^3/_4\,\mu_s$	1.9	3.0	4.6
	μ_s	1.7	2.4	3.9

Table 3: Obtained speed-ups for proposed TripleA approaches using LG/QSW feature extraction compared to the baseline systems (speed-up calculation is based on the median time per comparison).

5 Conclusions

We have presented and evaluated a new method (*TripleA*) for speeding up *HD* comparisons with rotation correction for iriscodes. This proposed method uses a screening process for the oscillating *HD* sequences under rotation which results in an up to four-fold speed-up. For two different feature extraction techniques operation points resulting in maximum speed-up, i.e. step-sizes of 4 to 5 for the static mode and $^3/_4\,\mu_s$ for the dynamic mode, coincide with the lowest impact in terms of loss of EER and FNMR at FMR=0.01%. *TripleA* can be used without further requirements and is compatible with binning and parallelization techniques making it widely applicable. To facilitate reproducible research an implementation of *TripleA* will be made available together with [19].

Further optimization of the first search step allows for fewer accurate searches and would further speed up the comparisons. In future work we will analyse the possibility of optimizing the first screening search by using multi-threading and the GPU.

Acknowledgements

This work was partially supported by the German Federal Ministry of Education and Research (BMBF) within the Center for Research in Security and Privacy (CRISP) and the Austrian Science Fund (FWF) project no. P27776.

References

[1] J. Daugman, "How iris recognition works," *Trans. on Circuits and Systems for Video Technology*, vol. 14, no. 1, pp. 21–30, 2004. DOI: 10.1109/ICIP.2002.1037952 (cit. on pp. 2, 4).

[2] C. Rathgeb, A. Uhl, and P. Wild, *Iris Recognition: From Segmentation to Template Security*, ser. Advances in Information Security. Springer Verlag, 2013, vol. 59 (cit. on pp. 2, 3).

[3] M. J. Burge and K. Bowyer, *Handbook of Iris Recognition (2nd edition)*. Springer-Verlag New York, Inc., 2016 (cit. on p. 2).

[4] A. Ross, "Iris recognition: The path forward," *Computer*, vol. 43, pp. 30–35, 2010. DOI: 10.1109/MC.2010.44 (cit. on p. 2).

[5] J. Daugman, "Information theory and the iriscode," *Trans. on Information Forensics and Security*, vol. 11, no. 2, pp. 400–409, Feb. 2016. DOI: 10.1109/TIFS.2015.2500196 (cit. on pp. 2, 4, 5).

[6] F. Hao, J. Daugman, and P. Zielinski, "A fast search algorithm for a large fuzzy database," *Trans. on Information Forensics and Security*, vol. 3, no. 2, pp. 203–212, 2008 (cit. on pp. 2, 3).

[7] R. Rakvic, B. Ulis, R. Broussard, R. Ives, and N. Steiner, "Parallelizing iris recognition," *Trans. on Information Forensics and Security*, vol. 4, no. 4, pp. 812–823, 2009 (cit. on p. 2).

[8] N. Vandal and M. Savvides, "CUDA accelerated iris template matching on graphics processing units (GPUs)," in *Proc 4th Int'l Conf. on Biometrics: Theory Applications and Systems (BTAS)*, 2010, pp. 1–7 (cit. on p. 2).

[9] J. Gentile, N. Ratha, and J. Connell, "An efficient, two-stage iris recognition system," in *Proc. 3rd Int'l Conf. on Biometrics: Theory, Applications, and Systems (BTAS)*, Sep. 2009, pp. 1–5 (cit. on pp. 2, 3).

[10] H. Proença, "Iris biometrics: Indexing and retrieving heavily degraded data," *Trans. on Information Forensics and Security*, vol. 8, no. 12, pp. 1975–1985, 2013 (cit. on p. 3).

[11] C. Rathgeb, F. Breitinger, H. Baier, and C. Busch, "Towards bloom filter-based indexing of iris biometric data," in *Proc. 8th Int'l Conf. on Biometrics (ICB)*, 2015, pp. 1–8 (cit. on p. 3).

[12] R. Mukherjee and A. Ross, "Indexing iris images.," in *Proc. Int'l Conf. on Pattern Recognition (ICPR)*, 2008, pp. 1–4 (cit. on p. 3).

[13] R. Gadde, D. Adjeroh, and A. Ross, "Indexing iris images using the burrows-wheeler transform," in *Proc. Int'l Workshop on Information Forensics and Security (WIFS)*, 2010, pp. 1–6 (cit. on p. 3).

[14] N. B. Puhan and N. Sudha, "Coarse indexing of iris database based on iris colour," *Int'l Journal on Biometrics*, vol. 3, no. 4, pp. 353–375, 2011, ISSN: 1755-8301 (cit. on p. 3).

[15] J. Fu, H. J. Caulfield, S.-M. Yooc, and V. Atluri, "Use of artificial color filtering to improve iris recognition and searching," *Pattern Recognition Letters*, vol. 26, no. 14, pp. 2244–2251, 2005 (cit. on p. 3).

[16] A. Dantcheva, P. Elia, and A. Ross, "What else does your biometric data reveal? a survey on soft biometrics," *Trans. on Information Forensics and Security*, vol. 11, no. 3, pp. 441–467, 2016 (cit. on p. 3).

[17] L. Masek, "Recognition of human iris patterns for biometric identification," Master's thesis, University of Western Australia, 2003 (cit. on p. 3).

[18] L. Ma, T. Tan, Y. Wang, and D. Zhang, "Efficient iris recognition by characterizing key local variations," *Trans. on Image Processing*, vol. 13, no. 6, pp. 739–750, 2004. DOI: 10.1109/TIP.2004.827237 (cit. on p. 3).

[19] *USIT – University of Salzburg iris toolkit*, http://www.wavelab.at/sources/Rathgeb16a, Version 2.0.x (cit. on pp. 3, 8).

[20] K. P. Hollingsworth, K. W. Bowyer, and P. J. Flynn, "The best bits in an iris code," *Trans. on Pattern Analysis and Machine Intelligence*, vol. 31, no. 6, pp. 964–973, 2009, ISSN: 0162-8828. DOI: http://dx.doi.org/10.1109/TPAMI.2008.185 (cit. on p. 4).

[21] Chinese Academy of Sciences' Institute of Automation, *Casia iris image database v4.0 — interval*, http://biometrics.idealtest.org, 2002 (cit. on p. 5).

[22] ISO/IEC TC JTC1 SC37 Biometrics, *Iso/iec 19795-1:2006. information technology – biometric performance testing and reporting – part 1: Principles and framework*, International Organization for Standardization and International Electrotechnical Committee, Mar. 2006, p. 56 (cit. on p. 5).